

This is the peer reviewed version of the following article:

Probing the Effect of Sildenafil on Progesterone and Testosterone Production by an Intracellular FRET/BRET Combined Approach / Casarini, L.; Riccetti, L.; Limoncella, Silvia; Lazzaretti, C.; Barbagallo, F.; Pacifico, S.; Guerrini, R.; Tagliavini, S.; Trenti, T.; Simoni, M.; Sola, M.; Di Rocco, G.. - In: BIOCHEMISTRY. - ISSN 0006-2960. - 58:6(2019), pp. 799-808. [10.1021/acs.biochem.8b01073]

Terms of use:

The terms and conditions for the reuse of this version of the manuscript are specified in the publishing policy. For all terms of use and more information see the publisher's website.

05/01/2026 18:40

Probing the effect of sildenafil on Progesterone and Testosterone production by an intracellular FRET/BRET combined approach

Livio Casarini^{1,2,§}, Laura Riccetti^{1,§}, Silvia Limoncella¹, Clara Lazzaretti¹, Federica Barbagallo³, Salvatore Pacifico⁴, Remo Guerrini⁴, Simonetta Tagliavini⁵, Tommaso Trenti⁵, Manuela Simoni^{1,2,6}, Marco Sola⁷, Giulia Di Rocco^{7,*}.

¹*Unit of Endocrinology, Department of Biomedical, Metabolic and Neural Sciences, University of Modena and Reggio Emilia, Modena, Italy.*

²*Center for Genome Research, University of Modena and Reggio Emilia, Modena, Italy.*

³*Department of Experimental Medicine University of Rome "La Sapienza", Rome, Italy.*

⁴*Department of Chemical and Pharmaceutical Sciences, University of Ferrara, Ferrara, Italy.*

⁵*Department of Laboratory Medicine and Pathological Anatomy, Azienda USL of Modena, Modena, Italy.*

⁶*Azienda, Ospedaliero-Universitaria di Modena, Modena, Italy.*

⁷*Department of Life Sciences, University of Modena and Reggio Emilia, Modena, Italy.*

*Correspondence: Giulia Di Rocco, Department of Life Sciences, University of Modena and Reggio Emilia, via G. Campi 103, 41125 - Modena, Italy. Phone: +39.0592058607. Email: giulia.dirocco@unimore.it.

§These authors contributed equally to this study.

Key words: sildenafil, PDE, steroidogenesis, cAMP, cGMP, biosensor

INTRODUCTION

Proteins and small organic molecules may be engineered for applications in molecular and cellular labeling, tracking, detection, drug delivery, medical imaging, and therapy for a personalized treatment of diseases¹⁻³. In this study we investigated molecular interactions mediating the synthesis of sex steroid hormones by Leydig cells through a recently developed FRET-labeled protein/substrate construct⁴ and BRET intracellular sensors^{5,6}. As many physiological processes, steroidogenesis is regulated by cyclic nucleotides (cNMPs) signaling systems and the control of cNMPs in mammalian cells is partly tailored by phosphodiesterases (PDEs) which are the cyclic nucleotide hydrolytic enzymes classified into 11 families⁷⁻¹⁰. Depending on their spatiotemporal distribution and active sites structure, many of the PDE's activities are modulated in response to a variety of signals including hormones, neurotransmitters, cytokines, light, and oxidative influence, contributing to the specificity and magnitude of cAMP and cGMP availability to its effectors⁹⁻¹³. Pathological conditions, such as erectile dysfunction and effect of lowering testosterone levels on aging¹⁴ may be ameliorated by selective PDE inhibitors, To this respect we focused on the PDE5

which specifically catalyzes the hydrolysis of cGMP to 5'-cGMP inactive¹⁵⁻¹⁷. PDE5's inhibitors succeed for therapy of erectile dysfunction, pulmonary hypertension, and cardiovascular diseases^{18,19}, where relaxation of smooth muscle is beneficial¹⁰; the inhibition of PDE5 activity impacts on steroidogenesis, since this enzyme acts as a modulator of intracellular cNMPs, regulating the downstream signaling cascade linked to hormone synthesis. It has been demonstrated that inhibition of PDE4, PDE8 and PDE5 enzymes significantly increases intracellular cNMPs concentration and production of testosterone by Leydig cells in the male^{12,20,21}. Testosterone is a sex steroid hormone produced by Leydig cell in the male. Steroidogenesis is stimulated by intracellular cNMPs increase, mainly cAMP, and starts from cholesterol conversion to intermediary products, such as pregnenolone and, subsequently, progesterone, culminating with the synthesis and release of testosterone^{22,23}. Production of this steroid is endogenously stimulated by the luteinizing hormone (LH), which, acting through its receptor (LHCGR), induces intracellular cAMP increase and transcription of genes encoding steroidogenic enzymes²⁴. In male infertility treatment, testosterone increase may be also stimulated by administration of exogenous choriogonadotropin (hCG), the pregnancy hormone binding LHCGR²⁴. cAMP is known as the main activator of the steroidogenic pathway, however, testosterone production may be increased upon use of cGMP-specific PDE5 inhibitors occurring *via* a not completely clear molecular mechanism^{25,26}.

In this study, FRET and BRET approaches are used to study the interaction of the PDE5-specific inhibitor (PDE5i) sildenafil with the human PDE5A2 catalytic subunit; the aim is to evaluate its activity in mediating cAMP/cGMP-dependent progesterone and testosterone synthesis (Figure 1) in live MLTC-1 (steroidogenic) and HEK293 cells.

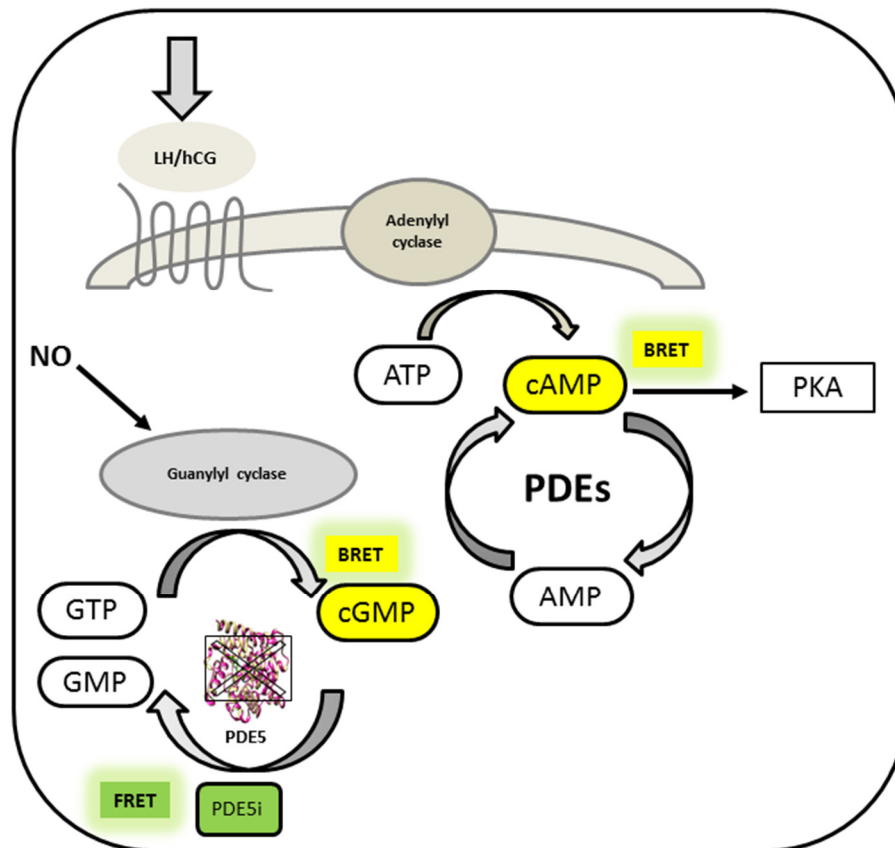


Figure1. *In cell* FRET/BRET monitoring approach of the Leydig cell steroidogenic pathway. Intracellular cGMP and cAMP increase is stimulated by LH or hCG administration and results in steroidogenic pathway activation and smooth muscle relaxation. cNMPs concentration is under the control of PDEs and may be modulated by PDE inhibitors. FRET and BRET biosensors were used for monitoring PD5i-PDE interaction, as well as cGMP and cAMP concentration in live cells.

Intracellular levels of the two cyclic second messengers were monitored by specific BRET sensors^{5,27–30} introduced and functional in live MLTC-1 and HEK293 cells. The detection of PDE5i was obtained through the FRET sensor (Figure 2)⁴ expressing *in vitro* the catalytic domain of hPDE5A2 (PDE5C) (identifier: O76074-2), tagged with a genetically encoded 6-amino-acid motif CCPGCC (TC) at the C terminus to be conjugated with FIAsh-EDT₂^{31–35} and a pseudo-substrate conjugated with rhodamine (cGMPS-rhodamine)⁴. This sensor was tested using sildenafil as a competitor.

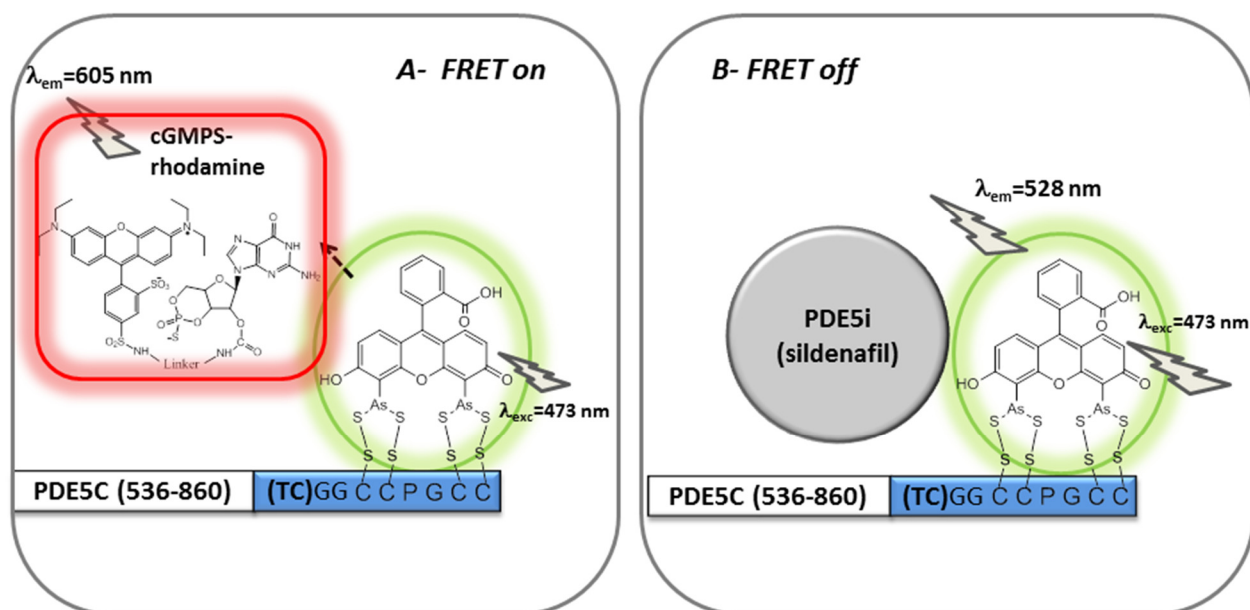


Figure 2. PDE5C-TC-FIAsH complex used for *in cell* FRET experiment. PDE5C-TC-FIAsH (Donor, D) and cGMPS-rhodamine (Acceptor, A) complexes are in the absence (panel -A) or in the presence of PDE5's inhibitors (panel-B). A) PDE5C (536-860)-encoding cDNA sequence was cloned into pDNA3.1, resulting in the PDE5 catalytic domain (yellow colored) fused with the teracysteine motif (light blue) able to conjugate the FIAsH compound (green highlighted) *via* As-S-Cys bond. The cGMPS-rhodamine serves as a pseudosubstrate (red highlighted) and is represented by the chemical formula. B) FRET signal decreases upon PDE5i competitive binding to the PDE5 catalytic domain.

In this paper we investigated the effect of PDE5i in modulating the LH/hCG-mediated signal transduction pathway, as well as the synthesis of progesterone and testosterone by a FRET/BRET-based method which allowed the multiple monitoring of biological interactors.

EXPERIMENTAL DETAILS

Plasmid vectors

Production of the PDE5 catalytic domain (residues 536-860) with a genetically encoded tetracysteine tag, was obtained using the *PDE5A2* cDNA sequence (UniProtKB - O76074 (PDE5A_HUMAN)) as a template and the following primers: **FW** : N-term 5'-ccaccatggcgggttctcatcatcatc-3'; **RVwt**:5'-ttagttccgcttggcctggc-3' and

RVTetrCys: -5'caggccaagcggaacGGTGGCTGTTGCCCGGGCTGCTGTGGTGGTtaa-3'. The amplified fragments for WT and TC *PDE5C* were first cloned into pTZ5ZR/T cloning vector and

then subcloned into the pDNA3.1 vector (Invitrogen) by a KpnI/BamHI double digestion. The right clones were then confirmed by DNA sequencing. Plasmidic DNA was obtained by using NucleoBond Xtra (Macherey-Nagel, Duren, Germany).

cGMPS-rhodamine synthesis

2'-(6-Aminohexylcarbamoyl)guanosine-3',5'-cyclic monophosphorothioate (RP-2'-AHC-cGMP) and the sulforhodamine B-X succinimidyl ester (Rhodamine Red-XTM) were purchased from BioLog (Hayward, CA, USA) and Thermo Fisher Scientific (Waltham, MA, USA) respectively. The solvents were purchased from Sigma-Aldrich (St. Louis, MO, USA). cGMPS-rhodamine was synthesized and purified as described previously⁴.

Recombinant gonadotropins

Human recombinant LH (Luveris®) and hCG (Ovitrelle®) were provided by Merck KGaA (Darmstadt, Germany).

Cell Culture and Transfection

Cell lines were cultured and handled as described previously³⁶. Briefly, HEK293 cells were grown in complete DMEM medium supplemented by 10% fetal bovine serum (FBS), 4.5 g/l glucose, 100 U/ml penicillin, 0.1 mg/ml streptomycin, and 1 mM glutamine (Invitrogen, Carlsbad, CA, USA). mLTC-1 cells (ATCC CRL-2065, LCG Standards, Molsheim, France) were grown in complete RPMI medium supplemented by 10% FBS, 100 U/ml penicillin, 0.1 mg/ml streptomycin, 1 mM glutamine and 1 mM HEPES. Transient transfections were performed in 96-well plate using Metafectene PRO (Biontex, München, Germany), following the manufacturer's protocol. To this purpose, 25 to 400 ng/well plasmid and 0.5 to 1.0 µl/well of Metafectene PRO were mixed in FBS-free medium and incubated 20 min. A 50 µl plasmid-Metafectene PRO mix was added to each wells containing 3×10^4 cells, in a total volume of 200 µl/well, and incubated 2 days before stimulation by gonadotropins and PDE5i.

Western blot analysis

HEK293 cells were lysed by an ice-cold aqueous buffer consisting in 50 mM HEPES, 10 mM MgCl₂, 100 mM NaCl, 10 mM β-glycerophosphate, 2 mM EGTA, 10% glycerol, 1% Triton-X-100, 1 mM phenylmethylsulfonyl fluoride, 10 µg/ml aprotinin, 10 µg/ml pepstatin, 10 µg/ml leupeptin, 0.1 mM sodium orthovanadate (all from Sigma-Aldrich). Lysates were purified by 10-min centrifugation at 12000 x g. Protein concentrations were estimated by colorimetric assay

(#5000001; Bio-Rad Laboratories, Hercules, CA, USA) based on the Bradford's protocol³⁷, and heated 5 min at 100°C in Laemmli buffer (Sigma-Aldrich) before electrophoresis. Proteins were separated by 10% SDS-PAGE gels and transferred to polyvinylidene fluoride membranes (Amersham Biosciences; GE Healthcare, Chicago, IL, USA) using blotting apparatus (Bio-Rad). Membranes were incubated overnight at 4 °C with the rabbit anti-PDE5A primary antibody (#sc-32884, 1:1000 dilution; Santa Cruz Biotechnology, Santa Cruz, CA, USA). After incubation with the horseradish peroxidase-conjugated anti-rabbit secondary antibody ((#NA9340V; GE Healthcare), signals were developed by the ECL reagent and detected by QuantityOne analysis software using the VersaDoc system (Bio-Rad Laboratories).

FRET plate reader data acquisition and analysis

3×10^4 cells/well HEK293 cells transiently expressing PDE5C-TC were seeded in duplicate into black-bottom 96-well plates (Greiner Bio-One GmbH, Kremsmünster, Austria) two days before experiments. Medium was replaced by 200 μ l PBS enriched by 1 mM CaCl_2 and 1 mM MgCl_2 . FAsH was then added directly to wells and measurements performed after 30 min at 20°C. For detection of PDE5C-TC-FAsH signals, samples were analyzed by the CLARIOstar plate reader (BMG Labtech, Offenburg, Germany). The monochromator was set to the wavelength of 473 ± 10 nm for excitation and 528 ± 14 nm for emission. cGMPS-rhodamine signals were analyzed at the wavelengths of 473 ± 10 and 605 ± 10 nm (excitation and emission, respectively). FRET analysis was performed at the wavelengths of $473/10$ nm for excitation, and at 528 ± 14 nm, the donor (D) and at 605 ± 10 nm, the acceptor (A) emissions, respectively. Direct ratiometric measurements were applied, using the A/D intensity ratio between cGMPS-rhodamine and PDE5CTC-FAsH. These procedures were applied after evaluating that the donor:acceptor stoichiometry is 1:1 in untransfected cells, after background signal subtraction. A background value of 3000 -4000 counts per seconds for HEK293 and of 12000-13000 counts per seconds for MLTC-1 was registered, and this was then subtracted each time. On the other hand the high-limit threshold at which the instrument it's able to read has been demonstrated to be 260000 counts per seconds. So we discarded the measurements containing these values, considering as good sets of data the ones with maximum intensities of 150000. Therefore we have adjusted the transfected amount of protein and of probes in order of being in that range.

FAsH staining and imaging

3×10^4 PDE5-TC-expressing HEK293 cells/well were plated in 24 multi-well plates. 48-h transfected cells were labelled for 10 min at 37°C by 10 μ M 1,2-ethanedithiol (EDT_2) and 0.1 μ M FAsH

(Thermo Fisher Scientific), diluted in HBSS (Sigma-Aldrich). Samples were washed twice by 250 μ M 1,2-ethanedithiol (EDT₂) diluted in HBSS. Cells were fixed by 10-min treatment using 4% paraformaldehyde, at room temperature (RT), then analyzed using an inverted TCS SP2 confocal microscope (Leica, Wetzlar, Germany) interfaced with an Ar Laser (488 nm/20 mW) and equipped with AOBS. Images were acquired at 63X magnification (HCX PL APO 63x/1.40 - oil - Lambda blue correction) and processed by LCS Lite (Leica). Samples were labelled for 10 min at 37°C with FIAsh-EDT₂ (0,5 μ M) in HBSS and washed twice in 150 μ M 1,2-ethanedithiol (EDT₂) in HBSS. Cells were fixed with 4% (w/v) paraformaldehyde for 15 min at RT and then imaged using an inverted *Leica TCS SP2* confocal microscope interfaced with an Ar Laser (488 nm/20 mW), equipped with AOBS and operated at a magnification of 63x (HCX PL APO 63x/1.40 - oil - Lambda blue correction).

Displacement experiments

Displacement experiments were performed using a fixed sildenafil concentration equimolar to the cGMPS-rhodamine constant (9 μ M-10 μ M). The complex PDE5C-TC-FIAsh/cGMPS-rhodamine was analyzed by signal acquisition at wavelengths of 528 \pm 10 nm and 605 \pm 10 nm (emissions), and at 473 \pm 10 nm (excitation), in the presence of 0.5 μ M sildenafil. A/D ratio variations were calculated, in the absence and in presence of sildenafil. Dose-response experiments were also performed following a similar procedure and by treating cells with increasing concentrations of sildenafil (0 pM-10 μ M range).

Evaluation of cAMP and cGMP production by BRET

BRET methods for evaluation of cAMP and cGMP recruitment were previously validated^{5,38}. Briefly, cAMP production was measured in live mLTC1 cells transiently expressing the BRET-based cAMP sensor CAMYEL^{6,36,38}. This molecule is an inactive cytosolic mutant form of the human exchange factor directly activated by cAMP 1 (EPAC1) fused with the Renilla luciferase (Rluc) and the green fluorescent protein (GFP). Upon stimulation by drug, cAMP binding to EPAC1 results in conformational rearrangements of the sensor, leading to a dose-dependent decrease of BRET signal occurring in the presence of coelenterazine H (Interchim, Montluçon, France), as a Rluc substrate.

cGMP production was evaluated in mLTC1 cells transiently expressing the GFP²-GAFa-Rluc sensor (provided by Dr Visweswariah, Indian Institute of Science, Bangalore, India)⁵. Intracellular cGMP binds the specific GAF domain, resulting in GFP²-GAFa-Rluc conformational changes and,

accordingly, in BRET signal increase. The detection range of the cGMP BRET biosensor was evaluated by dose-response experiments using 8-br-cGMP as a standard (Supplementary figure 1). For both cAMP and cGMP assays, MLTC-1 cells were suspended in 40 μ l/well of 1X PBS and 1 mM HEPES. Cells were incubated 20 min with increasing doses of sildenafil (1 pM-1 μ M range), then washed and stimulated 30 min at 37 °C with a fixed dose of hCG or LH (590 pM LH; 67 pM hCG). These gonadotropin doses consist in the 50% effective concentration (EC₅₀) calculated previously on cAMP production using different cell models, including the MLTC-1 cell line^{36,39,40}. BRET measurements were performed upon addition of 10 μ l/well of 5 μ M Coelenterazine H, using the CLARIOstar plate reader (BMG Labtech).

Evaluation of progesterone and testosterone synthesis

5 \times 10⁴ MLTC-1 cells/well were seeded in 24-well plates and serum starved 12 h before treatments. Cells were treated 20 min by increasing concentration of sildenafil (1 pM-1 μ M range), then washed and incubated 8 or 24 h with 590 pM LH or 67 pM hCG. Reactions were blocked by immediate freezing of the samples at -80°C, then total progesterone and testosterone was measured in the supernatants by immunoassay using an ARCHITECT analyser (Abbot Diagnostics, Chicago, IL, USA).

Statistical analyses.

Values were indicated as means \pm SEM and fitted using nonlinear regressions. Comparisons were performed by Mann-Whitney's U-test- and two-way ANOVA, as appropriated, using the GraphPad Prism software (San Diego, CA, USA). Differences were taken as significant for p<0.05.

RESULTS AND DISCUSSION

Protein conjugation in live cells

To carry out an *in vitro* FRET study on PDE5C-TC-FlAsH/cGMPS-rhodamine complex, a preliminary characterization of the single emission intensities of the donor ((D)-FlAsH) and the acceptor ((A)-rhodamine) was performed^{4,41}. The kinetics of FlAsH binding to PDE5C-TC, expressed both in HEK293 and in MLTC-1 Leydig tumor cell, was evaluated. The fluorescence intensity of FlAsH alone was measured over one hour (Figure 3A), indicating basal, and background emission. The signals were recorded using the excitation wavelength of 473 nm and two emission filters: 528 \pm 10 nm; 605 \pm 10 nm which represented the experimental conditions for the

subsequent FRET measurements. Both FAsH emissions at 528 nm reached a threshold after 30-40 min³² which was then used as incubation time in all measurements (Figure 3). The acceptor alone displayed the expected zero emission at 528 nm and a minimal stable emission at 605 nm due to the *non-zero* contribution of the direct excitation at the 473 nm wavelength (data not shown). Confocal images confirmed that the tetracysteine tag, fused to the C-terminus of the catalytic domain of PDE5 (PDE5C-TC), led to free cytosolic distribution of the fluorescent protein upon FAsH probe binding (Figure 3B). Cells labeled with FAsH were excited at 473 nm and emission was detected in the 530–600 nm wavelength range (i.e., FAsH fluorescence), while cells expressing the PDE5 catalytic domain lacking the tetracysteine tag (PDE5C WT) showed nonspecific, background signals, likely due to other cysteine motifs of cellular origin (Figure 3B).

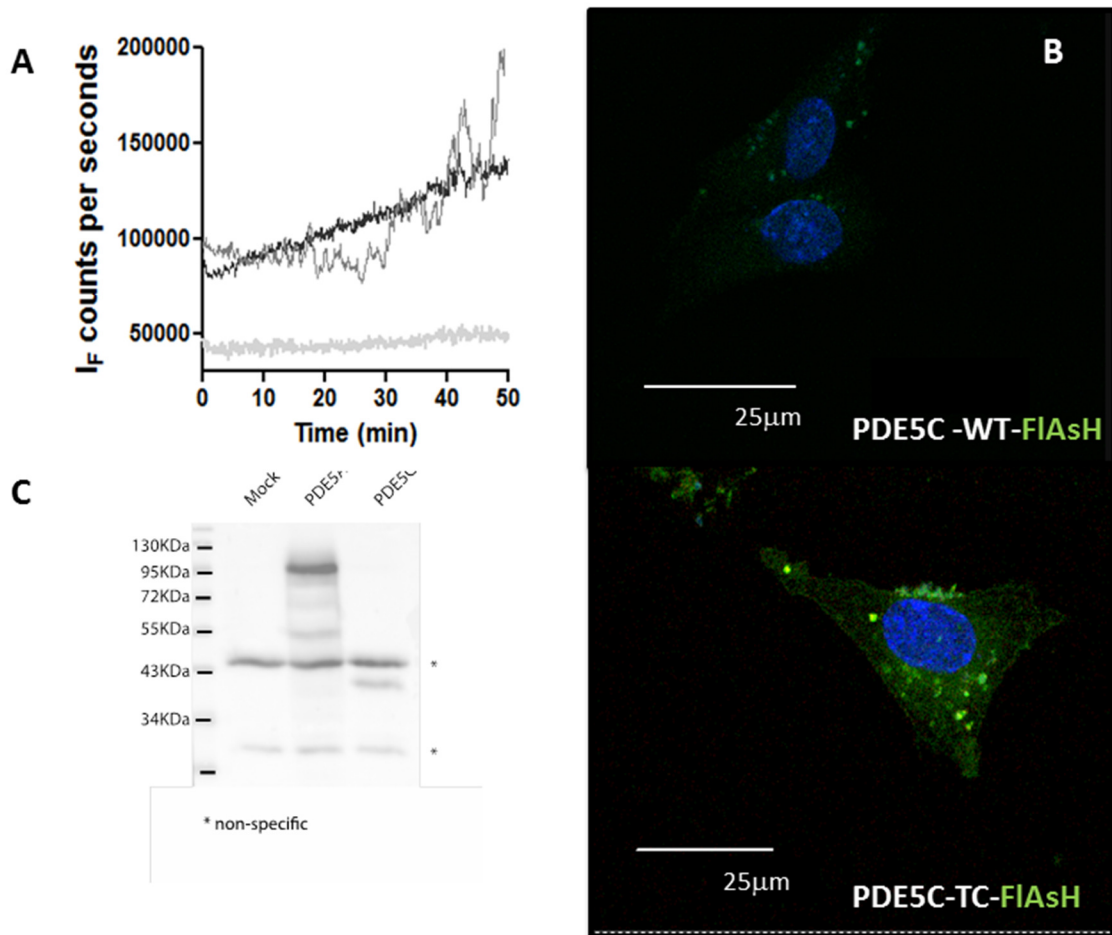


Figure 3. Analysis of PDE5C and FAsH functioning. A) Time-course of FAsH-EDT₂ (0,5 μM) binding to PDE5C-TC (λ_{exc} = 473 nm, λ_{em} = 528 nm) in HEK293 (grey line) and mLTC-1 (black line) cell lines. In light grey is reported the PBS signal (control). B) Confocal images of HEK293 transfected using 50 ng of PDE5C-TC and PDE5C WT cDNA. Nuclei staining with DAPI (blue) is

shown. The white scale bar = 25 μm . C) Western Blot analysis, using anti-PDE5 antibody, of HEK293 cells extracts transfected with an empty expression vector (line 1), p3xflag hPDE5A2 (line 2) or pcDNA3 PDE5C-TC (line 3). Asterisks indicates nonspecific band.

FRET validation

Assessment of FRET couple efficiency from the donor FIAsh (D) to the acceptor rhodamine (A) was performed in PDE5C-TC-expressing HEK293 cells. Donor emission quenching upon initial excitation and the concomitant increase in acceptor emission intensity were evaluated over 40 min (Figure 4). To this purpose, 25 ng/well of PDE5C-TC cDNA were used for cell transfection before both FIAsh and cGMPS-rhodamine addition. FIAsh-EDT₂ or cGMPS-rhodamine alone were added in control wells (Figure 4) and emissions were overall constant over time, thereby confirming the occurrence of a stable FRET in live cells.

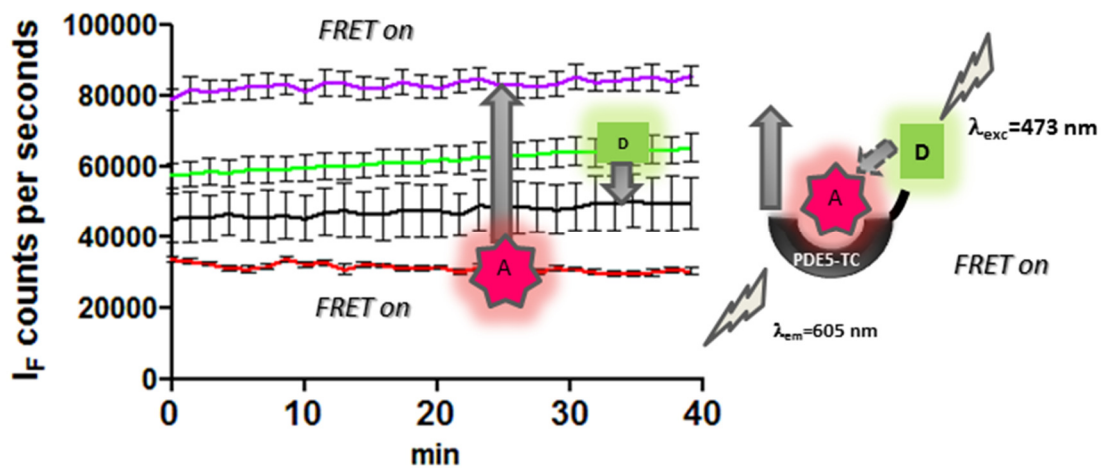


Figure 4. Time-course analysis and validation of FRET from FIAsh-EDT₂ to cGMPS-rhodamine in live, PDE5C-TC-expressing HEK293 cells. Emission intensity of the acceptor (A) increases upon spatial proximity between the cGMPS-rhodamine (A) and the donor FIAsh (D) bound to the PDE5-TC. Fluorescence intensity (average value; 24 replicates) of the acceptor alone (cGMPS-rhodamine, red line; filter $\lambda_{\text{exc}}=473/10$ nm; $\lambda_{\text{em}}=605/10$ nm), donor alone (PDE5C-TC-FIAsh, green line; filter $\lambda_{\text{exc}}=473/10$ nm; $\lambda_{\text{em}}=528/10$ nm) FRET donor (black line; filter $\lambda_{\text{exc}}=473/10$ nm; $\lambda_{\text{em}}=528/10$ nm) and FRET acceptor (violet line; filter $\lambda_{\text{exc}}=473/10$ nm; $\lambda_{\text{em}}=605/10$ nm). FIAsh 0,5 μM and cGMPS-rhodamine 9 μM .

Dose-dependent FRET measurements were performed to measure labeled PDE5-TC and cGMP binding affinity. To this purpose, both PDE5C-TC-expressing HEK293 and MLTC-1 cells were used, while cells transfected using the PDE5C-WT expressing cDNA served as a negative control. FRET was induced upon 30 min incubation by 0.5 μ M FIAsh, excited by light at $\lambda_{exc}=473\pm10$ nm, then titrated using increasing amounts of cGMPS-rhodamine (0-18 μ M range, figure 5A; 0-25 μ M range; figure 5B). Preferential excitation of FIAsh ($\lambda_{exc} = 473$ nm), with maximum at 528 nm, (D) triggered excitation energy-transfer to rhodamine leading to subsequent light emission at 605 nm (A) wavelength indicating the formation of the PDE5C-TC-FIAsh/cGMPS-rhodamine complex. This molecular interaction was demonstrated by the increase of the A/D ratio occurring together with the increase of the cGMPS-rhodamine concentration, following a Hill trend (Figure 5A and 5B). In Figure 5A data are represented by a hyperbole consistent with 1: 1 enzyme-ligand binding, while in Figure 5B the trend has a sigmoidal distribution. Since we know that both constructs have the same stoichiometry, the sigmoidal shape of the curve obtained by data distribution from MLTC-1 cells (Fig 5B) could be due to the presence of endogenous PDE5⁴² competing to the binding of the PDE5C-TC to cGMPS-rhodamine and causing a delay, at first. The A/D values were normalized subtracting the background signal of untransfected cells. While data distribution obtained by TC-tagged protein-expressing cells yielded a binding curve, data from WT PDE5C-expressing cells resulted in Lambert-Beer trend together with cGMPS-rhodamine increase. Since the donor:acceptor stoichiometry is 1:1, best fitting affinity constant values (K_d) of 5.6 ± 3.2 μ M and 13.7 ± 0.8 μ M were obtained from HEK293 and MLTC-1 cells, respectively. These K_d values are similar to that of full-length PDE5A and in agreement with what previously demonstrated using the purified form of the same construct^{4,8}. The moderate affinities ($K_d=5,6$ μ M (HEK293); $K_d=13,7\mu$ M (MLTC-1)) resulted in a dose-response relationship that matched physiological cGMP affinity for PDE5A (Fig 5 A,B). The use of the catalytic domain instead of the full-length protein avoided stoichiometry-related problems since the catalytic unit binds only one substrate molecule. Moreover, using FIAsh and a cGMP-conjugated pseudo-substrate avoided problems of unbalanced expressions between donor and acceptor which hamper quantitative analyses of FRET changes. However, the problem of the rhodamine direct excitation cannot be avoided, but it was confined optimizing the experimental conditions. ($\lambda_{exc}=473$ nm instead of 503nm; cleft width =10 nm instead of 14 nm).

Moreover, these data demonstrate that such a construct may be successfully used for evaluating the potency of PDE5 competitive inhibitors in live cells.

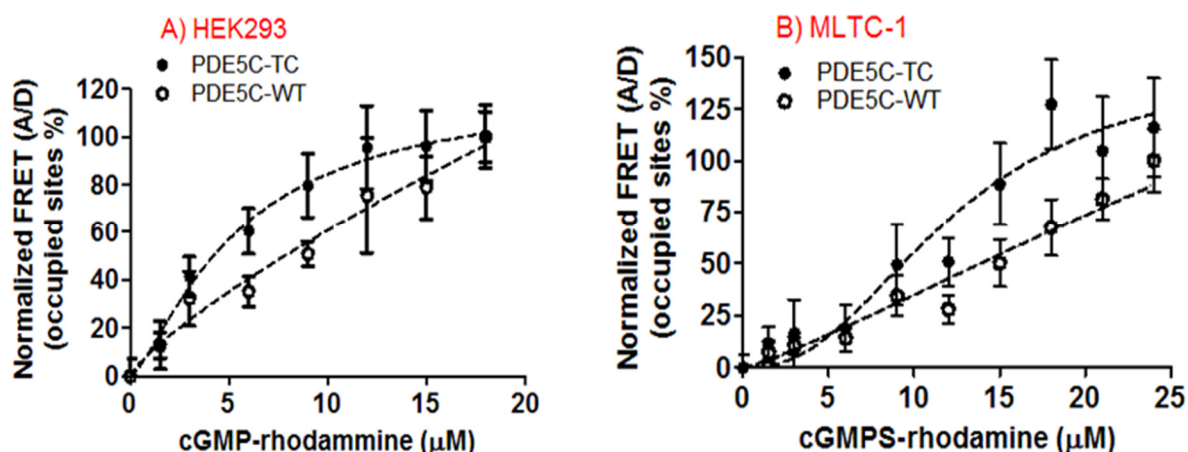


Figure 5. Hill plots for PDE5C-TC-FIAsH/cGMPS-rhodamine complex formation in live A) HEK293 and B) MLTC-1 cells. The normalized FRET-A/D ratio represented the fraction of occupied PDE5C-TC-FIAsH (●) and PDE5C lacking the TC tag (○) binding sites upon increasing aliquots of cGMPS-rhodamine; means±standard error of mean (SEM); n=4. Data of TC-tagged protein-expressing cells resulted in K_d values of $5.6 \pm 3.2 \mu\text{M}$ (HEK293 cells) and $13.7 \pm 0.8 \mu\text{M}$ (MLTC-1 cells), calculated using the GraphPad Prism software (GraphPad Software Inc., San Diego, CA), while no K_d s can be calculated from data represented by Lambert-Beer trends obtained by WT PDE5C-expressing cells.

FRET switched off by PDE5i

The live monitoring of cNMPs at the intracellular level may be a useful tool for understanding PDE5i functioning and the regulation of multiple intracellular events, leading to relevant clinical implications. In this paper, a new FRET tool based on a protein-conjugated/substrate-conjugated construct was developed for real-time evaluation of the intracellular action of sildenafil. The study showed that PDE5C-TC-FIAsH and cGMP-rhodamine conjugates were ideally suited to act jointly as a PDE5i sensor, enabling detection of sildenafil in a reliable and rapid manner. Once established the binding, the FRET displacement was investigated, treating the cells by pM-μM concentrations of sildenafil, in the presence or in the absence of LH and hCG, as molecules used for infertility treatment^{24,43}. Efficiency of the PDE5i sildenafil in replacing cGMPS-rhodamine to the PDE5C-TC-FIAsH was evaluated. Since sildenafil has higher binding affinity to PDE5 than cGMP, the FRET measured as a A/D ratio (Figure 5) should decrease in the presence of increasing concentrations of the competitor (pM-μM range) which replaces the PDE5-cGMP binding. Results obtained by the

analysis of the PDE5C-TC-FIAsH/cGMPS-rhodamine complex (Figure 5) served to calculate cGMPS-rhodamine concentrations, resulting in about 50-60% FRET efficiency, to be used as fixed doses in displacement experiments (9.0 μ M in HEK293 cells; 10 μ M in MLTC-1 cells).

Results indicated decrease of FIAsH-to-rhodamine FRET efficiency (A/D ratio), demonstrating displacement of cGMPS-rhodamine from the PDE5-TC-FIAsH by sildenafil (Figure 6). Dose-dependent measurements were conducted for both the PDE5C-TC-expressing cell lines in the same experimental conditions and PDE5i inhibition constants (K_i) were calculated. Sildenafil K_i values were 3.6 ± 0.3 nM ($IC_{50} = 2.3$ nM) in live HEK293 cells (Figure 6A) and 10 ± 1.0 nM ($IC_{50} = 3.9$ nM) in live MLTC-1 cells (Fig 6B), corroborating previous observations¹³ and validating the sensor. The best-fitting curves were obtained using the following equation:

$$FRET = FRET_{min} + \frac{\Delta FRET}{1 + \left(\frac{IC_{50}}{[sildenafil]} \right)^{Hill\ slope}}$$

where $FRET_{min}$ is the minimum value at which the A/D ratio tends upon competitor's addition. The Hill slope resulted to be lower than 1.0, indicative of negative cooperativity due to decreased cGMP binding affinity possibly due to the binding of sildenafil to the PDE5's catalytic domain without displacing completely the pseudo-substrate.

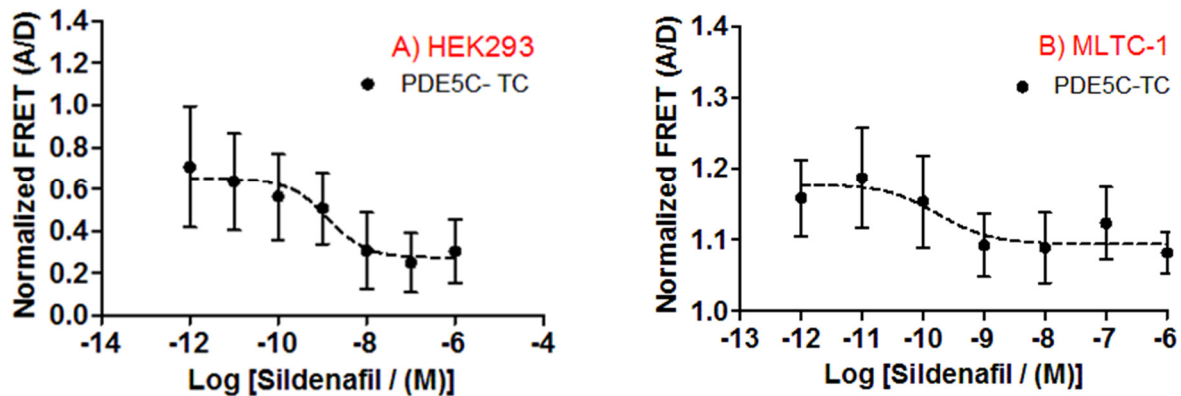


Figure 6. Displacement of cGMP from PDE5 by sildenafil in live HEK293 and MLTC-1 cells. A fixed dose of cGMPS-rhodamine, dependent on the cell model, was used and A/D ratios (FRET changes) were graphically represented against sildenafil concentrations (pM- μ M range). Data were means \pm SEM. A) PDE5C-TC-expressing HEK293 cells. 9 μ M cGMPS-rhodamine was used and plot lines were computed with the best-fitting value of $K_i = 3.6 \pm 0.3$ nM (n=5). B) PDE5C-TC-

expressing mLTC1 steroidogenic cells, in the presence of 10 μ M cGMPS-rhodamine. Plot lines are computed with the best-fitting value of $K_i=10\pm1.0$ nM (n=6).

The K_i values measured here perfectly matched the literature data¹³ (Figure 6 A and B). To the best of our knowledge, these FRET data in these cell lines are unprecedented.

cAMP and cGMP level monitoring in live MLTC-1 steroidogenic cells

Targeting LHCGR expressed in the Leydig cells, LH regulates the synthesis of sex steroid hormones in the male via cNMPs. Therefore, the evaluation of cNMPs levels after cell treatment by LH/hCG allowed assessment of the relationship between sildenafil treatment and testosterone production *in vitro*.

In Leydig cells, LH/hCG-dependent intracellular cNMPs increase, especially cAMP, is linked to the activation of the steroidogenic cascade culminating with testosterone production. Since PDE5-cGMP specific inhibition (Figure 6) may induce both intracellular cGMP and cAMP accumulation²⁶, the impact of PDE5i on both intracellular cGMP and cAMP levels was evaluated using BRET techniques^{5,6,38} in the mouse Leydig MLTC-1 cell line. To better mimic the *in vivo* exposure of Leydig cells to gonadotropins, MLTC-1 were treated by equipotent concentrations of gonadotropins³⁹, i.e. 590 pM LH and 67 pM hCG, to promote 3-h cNMPs production in the presence of sildenafil (pM- μ M range). Results were compared with those obtained from cells maintained in the absence of gonadotropin (Figure 7).

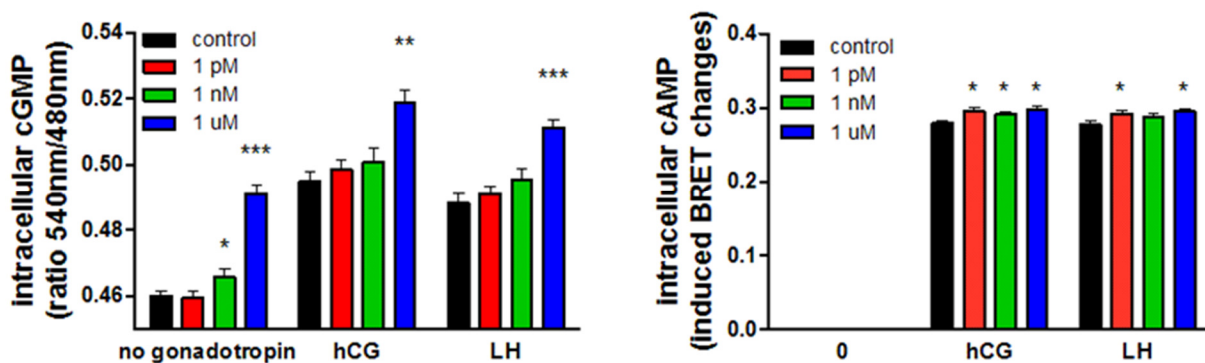


Figure 7: Intracellular cGMP and cAMP increase in sildenafil-treated mLTC1 cells. 25×10^4 cells/well were maintained 3 hours in the presence of pM- μ M concentrations of the PDE5i before addition of 590 pM LH or 67 pM hCG. 3-h cGMP and cAMP production were evaluated by BRET. Data are represented as mean \pm SEM. A) cGMP levels (n=6). B) cAMP levels (n=4). Differences

were considered significant for $p < 0.05$ (Mann-Whitney's *U*-test). Differences were considered *versus* the control condition of the same gonadotropin treatment (* $p < 0.05$, ** $p < 0.001$, *** $p < 0.0001$, respectively).

In MLTC-1 cells, both LH and hCG treatments induced both intracellular cGMP and cAMP increase, not depending on the presence of sildenafil (two-way ANOVA; $p < 0.05$; $n = 5-6$). In the absence of gonadotropins, cell treatment by PDE5i increased intracellular cGMP, consistently with the inhibition of PDE5-cGMP binding upon 1 μ M sildenafil addition (Figure 6) and with published data¹³. Interestingly, while cAMP production is not sildenafil concentration-dependent, the cyclic nucleotide significantly increased at the relatively very low LH/hCG concentration of 1 pM (1 pM; two-way ANOVA; $p < 0.05$; $n = 5-6$) compared to what described previously in MLTC-1 cells³⁶. This could be due to: i) the presence of increased amounts of cGMP promotes the production of cAMP ii) sildenafil inhibits also a cAMP-specific PDE causing a further increase in the cNMP levels and /or iii) both PDE2 and PDE3 are targeted by increasing amount of cGMP⁴⁴, resulting in cAMP increase detectable under gonadotropin treatment.

Evaluation of progesterone and testosterone synthesis

The role of cNMPs in inducing steroid production was determined as progesterone and testosterone levels by immunoassay. Effects of PDE5 inhibition on steroidogenesis were evaluated. To this purpose, 24-h production of testosterone and of its precursor progesterone was evaluated in cell media of 590 pM LH- or 67 pM hCG-treated mLTC1 cells, not depending on the presence of pM- μ M concentrations of sildenafil (Figure 8). No progesterone synthesis occurred in the absence of LH/hCG compared to sildenafil-untreated cells (basal), even in the presence of the PDE5i (two-way ANOVA and Bonferroni post-tests; $p \geq 0.05$; $n = 5$). Both gonadotropins induced the synthesis of progesterone (Fig. 8A), as a precursor of testosterone ($p < 0.05$; two-way ANOVA and Bonferroni post-tests; $n = 5$), progesterone levels did not increase upon addition of pM- μ M doses of PDE5i ($p \geq 0.05$; two-way ANOVA and Bonferroni post-tests; $n = 5$). Reflecting progesterone synthesis, testosterone production is detectable only in gonadotropin-treated MLTC-1 cells (Figure 8B; $p < 0.05$; Mann-Whitney's *U*-test; $n = 5$), while cell treatment by PDE5i failed in inducing steroidogenesis ($p \geq 0.05$; two-way ANOVA and Bonferroni post-tests; $n = 5$). Sildenafil significantly increased hCG-, but not LH-dependent testosterone production in a dose-dependent manner ($p < 0.05$; two-way ANOVA and Bonferroni post-tests; $n = 5$). Therefore inhibition of the NO-cGMP

signaling pathway does not increase the progesterone levels, but favors the production of testosterone starting from progesterone conversion (two-way ANOVA; $p < 0.05$; $n = 3$).

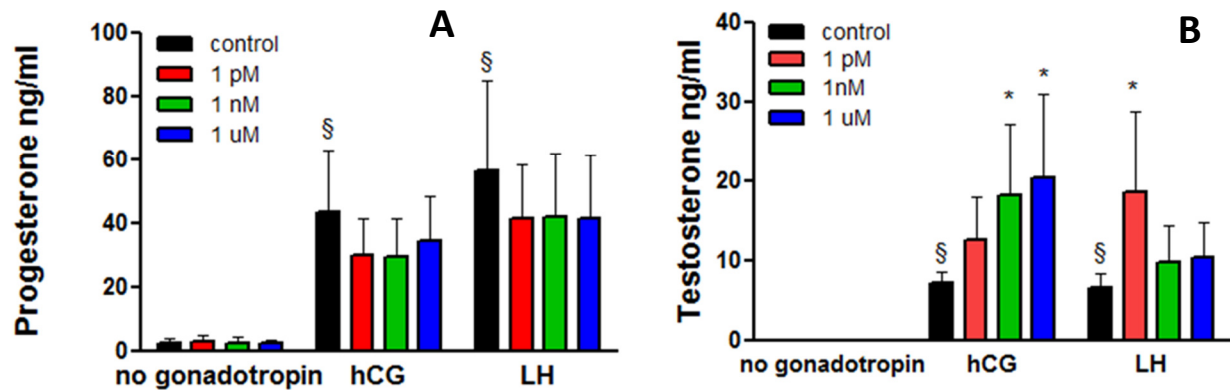


Figure 8. Measurement of LH/hCG-induced progesterone (A) and testosterone (B) production, in sildenafil-treated MLTC-1 cells. Samples were treated by 590 pM LH or 67 pM hCG, in the presence or in the absence of pM- μ M concentrations of sildenafil. Reactions were blocked by freezing cells 24-h at -80°C , total progesterone and testosterone levels were measured by immunometric assay. Data are represented as means \pm SEM. Differences were considered as significant for $p < 0.05$ ($n = 5$). *=significantly different *versus* control of same treatment using two-way ANOVA and Bonferroni post-tests; §=significantly different *versus* control/no gonadotropin condition using Mann-Whitney's *U*-test.

Our results confirmed that the interaction between the catalytic subunit of the PDE5 enzyme and cGMP was inhibited by sildenafil. These data reflected the PDE5i dose-dependence of cGMP accumulation in the mouse Leydig cell line (Figure 7). Interestingly, no cAMP accumulation was detected by the selective PDE5 inhibition *per se*, contrary to what previously demonstrated in isolated segments of human *corpus cavernosum* and cardiac muscle⁴⁵, suggesting that PDE5i action may be cell-specific. In MLTC-1 cells, both cGMP and cAMP increased under LH/hCG treatment. However, since no progesterone and testosterone production occurred in the absence of the hormones, in spite of high cGMP levels (Figure 7A), these data confirmed that gonadotropins are required to mediate Leydig cell steroidogenesis *via* cAMP. Indeed, genetic mutations depleting LH functions impair testosterone production and are causative of male infertility⁴⁶. However, cGMP may act as a modulator of the cAMP-dependent steroidogenic pathway, in LH/hCG-treated MLTC-1 cells, we found that progesterone levels are higher in the absence of sildenafil, likely as an effect of its conversion to testosterone (Figure 8). In this case, testosterone synthesis may be enhanced by selective PDE5 inhibition. In fact, previous findings demonstrated that the nitric oxide-cGMP signaling pathway and androgen production are connected *in vivo*^{25,47}.

Finally, it is worthy of note that the sildenafil dose-dependent increase of testosterone synthesis occurred in hCG-, but not in LH-treated cells (Figure 8B). Although hCG is the pregnancy hormone exclusive of female primates, it binds the mouse LH receptor and is used for male infertility treatment²⁴. Since hCG is known to have higher steroidogenic potential than LH^{24,48,49}, the impact of these two hormones on testosterone production may be different, at least in the presence of sildenafil. Recent studies focused on long- and short-term inhibition by sildenafil *in vivo*, demonstrated increase of circulating levels of testosterone due to coordinative stimulatory effect of cAMP and cGMP action^{12,20,21,30,50}, thus confirming the reliability of our new approach.

CONCLUSION

The FRET-based sensor described here proved to be a valuable tool for detecting binding of small molecules to the catalytic pocket of PDE5A. The approach is based on competitive displacement experiments. The observables are the emission intensities of an electronic excitation energy pair, namely FAsH (donor) that binds tetracysteine tagged proteins and rhodamine (acceptor) covalently bound to a non-reactive substrate analogue of this enzyme, cGMPS. FRET experiments proved, for the first time, the binding of the catalytic domain of PDE5A to a cGMPS-rhodamine conjugate in two different cellular environments (HEK293 and MLTC-1). The monitoring of cAMP and cGMP by BRET allowed exploitation of PDE5i effects on steroidogenesis, evaluating both NO-cGMP-mediated and cAMP-mediated pathways. Results indicated that sildenafil enhanced the gonadotropin-induced progesterone-to-testosterone conversion in a cAMP-independent manner, thus confirming previous *in vivo* findings not completely supported by *in vitro* data. The demonstration of sildenafil dose-dependence of intracellular cGMP accumulation confirmed the PDE5i efficacy in steroidogenic cells. This combined FRET/BRET approach used for live monitoring of cNMPs-mediated processes may be applied to compare the activity of several PDE5 inhibitors. Moreover, this method may be used to evaluate the effects of PDE5i on other intracellular pathways regulating endothelial functions, such as intracellular calcium ions increase

51.

Acknowledgments

The authors are grateful to Dr. Ilaria Martinelli for the preliminar procedures of PDE5C-TC cloning and to Prof. Glaucio Ponterini for helpful discussions on FRET theory and experimental data interpretation.

This work was supported by MIUR, Ministero dell'Istruzione, dell'Università e della Ricerca [FIRB grant; project RBFR12FI27 005 to Giulia Di Rocco]; by Fondo di Ateneo per la Ricerca [FAR2015 to Giulia Di Rocco] and by a grant to the Department of Biomedical, Metabolic and Neural Sciences (University of Modena and Reggio Emilia (Italy) in the Departments of Excellence Programme supported by MIUR. Authors thanks also the programme "Progetti di Rilevante Interesse Nazionale" (PRIN).

REFERENCES

- (1) Cai, W., and Chen, X. (2007) Nanoplatfoms for targeted molecular imaging in living subjects. *Small* 3, 1840–1854.
- (2) Godin, B., Sakamoto, J. H., Serda, R. E., Grattoni, A., Bouamrani, A., and Ferrari, M. (2010) Emerging applications of nanomedicine for the diagnosis and treatment of cardiovascular diseases. *Trends Pharmacol. Sci.* 31, 199–205.
- (3) Scaletti, F., Hardie, J., Lee, Y.-W., Luther, D. C., Ray, M., and Rotello, V. M. (2018) Protein delivery into cells using inorganic nanoparticle–protein supramolecular assemblies. *Chem. Soc. Rev.* 3421–3432.
- (4) Di Rocco, G., Martinelli, I., Pacifico, S., Guerrini, R., Cichero, E., Fossa, P., Franchini, S., Cardarelli, S., Giorgi, M., Sola, M., and Ponterini, G. (2018) Fluorometric detection of protein-ligand engagement: The case of phosphodiesterase5. *J. Pharm. Biomed. Anal.* 149, 335–342.
- (5) Biswas, K. H., Sopory, S., and Visweswariah, S. S. (2008) The GAF domain of the cGMP-binding, cGMP-specific phosphodiesterase (PDE5) is a sensor and a sink for cGMP. *Biochemistry* 47, 3534–3543.
- (6) Jiang, L. I., Collins, J., Davis, R., Lin, K., Decamp, D., Hsueh, R., Rebres, R. a, Ross, E. M., Taussig, R., and Sternweis, P. C. (2008) NIH Public Access 282, 10576–10584.
- (7) Maurice, D. H., Ke, H., Ahmad, F., Wang, Y., Chung, J., and Manganiello, V. C. (2014) Advances in targeting cyclic nucleotide phosphodiesterases. *Nat. Rev. Drug Discov.* 13, 290–314.
- (8) Bender, A. T. (2006) Cyclic Nucleotide Phosphodiesterases: Molecular Regulation to Clinical Use. *Pharmacol. Rev.* 58, 488–520.
- (9) Conti, M., and Beavo, J. (2007) Biochemistry and Physiology of Cyclic Nucleotide Phosphodiesterases: Essential Components in Cyclic Nucleotide Signaling. *Annu. Rev. Biochem.* 76, 481–511.
- (10) Keravis, T., and Lugnier, C. (2012) Cyclic nucleotide phosphodiesterase (PDE) isozymes as targets of the intracellular signalling network: Benefits of PDE inhibitors in various diseases and perspectives for future therapeutic developments. *Br. J. Pharmacol.* 165, 1288–1305.
- (11) Francis, S., Blount, M., and Corbin, J. (2011) Mammalian cyclic nucleotide phosphodiesterases: molecular mechanisms and physiological functions. *Physiol. Rev.* 91, 651–690.
- (12) Shimizu-Albergine, M., Tsai, L.-C. L., Patrucco, E., and Beavo, J. A. (2012) cAMP-Specific Phosphodiesterases 8A and 8B, Essential Regulators of Leydig Cell Steroidogenesis. *Mol. Pharmacol.* 81, 556–566.
- (13) Corbin, J. D., and Francis, S. H. (1999) Cyclic GMP phosphodiesterase-5: Target of sildenafil. *J. Biol. Chem.* 274, 13729–13732.
- (14) Mokry, J., Urbanova, A., Medvedova, I., Kertys, M., Mikolka, P., Kosutova, P., and Mokra, D. (2017) Effects of tadalafil (PDE5 inhibitor) and roflumilast (PDE4 inhibitor) on airway reactivity and markers of inflammation in ovalbumin-induced airway hyperresponsiveness in guinea pigs. *J. Physiol. Pharmacol.* 68, 721–730.
- (15) Card, G. L., England, B. P., Suzuki, Y., Fong, D., Powell, B., Lee, B., Luu, C., Tabrizizad, M., Gillette, S., Ibrahim, P. N., Artis, D. R., Bollag, G., Milburn, M. V., Kim, S. H., Schlessinger, J., and Zhang, K. Y. J. (2004) Structural basis for the activity of drugs that inhibit phosphodiesterases. *Structure* 12, 2233–2247.
- (16) Zhang, K. Y. J., Card, G. L., Suzuki, Y., Artis, D. R., Fong, D., Gillette, S., Hsieh, D., Neiman, J., West, B. L., Zhang, C., Milburn, M. V., Kim, S., Schlessinger, J., Bollag, G., and Haven, N. (2004) Short Article for Nucleotide Selectivity by Phosphodiesterases 15, 279–286.
- (17) Huai, Q., Liu, Y., Francis, S. H., Corbin, J. D., and Ke, H. (2004) Crystal Structures of Phosphodiesterases 4 and 5 in Complex with Inhibitor 3-Isobutyl-1-methylxanthine Suggest a Conformation Determinant of Inhibitor Selectivity. *J. Biol. Chem.* 279, 13095–13101.
- (18) Giannetta, E., Isidori, A. M., Galea, N., Carbone, I., Mandosi, E., Vizza, C. D., Naro, F., Morano, S., Fedele, F., and Lenzi, A. (2012) Chronic inhibition of cGMP phosphodiesterase 5A

- improves diabetic cardiomyopathy: A randomized, controlled clinical trial using magnetic resonance imaging with myocardial tagging. *Circulation* 125, 2323–2333.
- (19) Spitzer M., Bhasin S., Travison TG, Davida MN, Stroh H, B. S. (2013) Sildenafil increases serum testosterone levels by a direct action on the testes. *Andrology* 1, 913–18.
- (20) Vasta, V., Shimizu-Albergine, M., and Beavo, J. A. (2006) Modulation of Leydig cell function by cyclic nucleotide phosphodiesterase 8A. *Proc. Natl. Acad. Sci. U. S. A.* 103, 19925–30.
- (21) Sokanovic, S. J., Capo, I., Medar, M. M., Andric, S. A., and Kostic, T. S. (2018) Long-term inhibition of PDE5 ameliorates aging-induced changes in rat testis. *Exp. Gerontol.* 108, 139–148.
- (22) Walter L. Millerc and Richard J. Auchus. (2011) The Molecular Biology, Biochemistry, and Physiology of Human Steroidogenesis and Its Disorders. *Endocr Rev.* 32, 81–151.
- (23) Flück, C. E., and Pandey, A. V. (2014) Steroidogenesis of the testis - new genes and pathways. *Ann. Endocrinol. (Paris).* 75, 40–47.
- (24) Casarini, L., Santi, D., Brigante, G., and Simoni, M. (2018) Two hormones for one receptor: evolution, biochemistry, actions and pathophysiology of LH and hCG. *Endocr. Rev.*
- (25) Belli, S., Santi, D., Leoni, E., Dall’Olio, E., Fanelli, F., Mezzullo, M., Pelusi, C., Roli, L., Tagliavini, S., Trenti, T., Granata, A. R., Pagotto, U., Pasquali, R., Rochira, V., Carani, C., and Simoni, M. (2016) Human chorionic gonadotropin stimulation gives evidence of differences in testicular steroidogenesis in Klinefelter syndrome, as assessed by liquid chromatography-tandem mass spectrometry. *Eur. J. Endocrinol.* 174, 801–811.
- (26) Saraiva, K. L. A., Silva, A. K. S. E., Wanderley, M. I., De Araújo, A. A., De Souza, J. R. B., and Peixoto, C. A. (2009) Chronic treatment with sildenafil stimulates Leydig cell and testosterone secretion. *Int. J. Exp. Pathol.* 90, 454–462.
- (27) Ponsioen, B., Zhao, J., Riedl, J., Zwartkruis, F., van der Krogt, G., Zaccolo, M., Moolenaar, W. H., Bos, J. L., and Jalink, K. (2004) Detecting cAMP-induced Epac activation by fluorescence resonance energy transfer: Epac as a novel cAMP indicator. *EMBO Rep.* 5, 1176–1180.
- (28) Nikolaev, V. O., Bünemann, M., Hein, L., Hannawacker, A., and Lohse, M. J. (2004) Novel single chain cAMP sensors for receptor-induced signal propagation. *J. Biol. Chem.* 279, 37215–37218.
- (29) Russwurm, M., Mullershausen, F., Friebe, A., Jäger, R., Russwurm, C., and Koesling, D. (2007) Design of fluorescence resonance energy transfer (FRET)-based cGMP indicators: a systematic approach. *Biochem. J.* 407, 69–77.
- (30) Andric, S. a, Janjic, M. M., Stojkov, N. J., and Kostic, T. S. (2010) Sildenafil treatment in vivo stimulates Leydig cell steroidogenesis via the cAMP/cGMP signaling pathway. *Am. J. Physiol. Endocrinol. Metab.* 299, E544-50.
- (31) Adams, S. R., Campbell, R. E., Gross, L. A., Martin, B. R., Walkup, G. K., Yao, Y., Llopis, J., and Tsien, R. Y. (2002) New biarsenical ligands and tetracysteine motifs for protein labeling *in vitro* and *in vivo*: synthesis and biological applications. *J Am Chem Soc* 124, 6063–6076.
- (32) Hoffmann, C., Gaietta, G., Adams, S. R., Terrilon, S., Ellisman, M. H., Tsien, R. Y., and Lohse, M. J. (2011) Fluorescent labelling of tetracysteine-tagged proteins in intact cells. *NIH Public Access* 5, 1666–1677.
- (33) Hannibal, L., Tomasina, F., Capdevila, D. A., Demicheli, V., Tórtora, V., Alvarez-Paggi, D., Jemmerson, R., Murgida, D. H., and Radi, R. (2016) Alternative Conformations of Cytochrome c: Structure, Function, and Detection. *Biochemistry* 55, 407–428.
- (34) Griffin, A. B., Adams, S. R., and Tsien, R. Y. (1998) Specific Covalent labeling of recombinant protein moelcules inside live cells. *Science (80-.).* 281, 269–272.
- (35) Adams, S. R., and Tsien, R. Y. (2008) Preparation of the membrane-permeant biarsenicals, FIAsh- EDT2 and ReAsH-EDT2 tagged proteins. *Nat Protoc* 3, 1527–1534.
- (36) Riccetti, L., Yvinec, R., Klett, D., Gallay, N., Combarous, Y., Reiter, E., Simoni, M., Casarini, L., and Ayoub, M. A. (2017) Human Luteinizing Hormone and Chorionic Gonadotropin Display Biased Agonism at the LH and LH/CG Receptors. *Sci. Rep.* 7, 1–11.
- (37) MM., B. (1976) A rapid and sensitive method for the quantitation of microgram quantities of

protein utilizing the principle of protein-dye binding. *Anal. Biochem* 7, 248–254.

(38) Ayoub, M. A., Landomiel, F., Gallay, N., Jégot, G., Poupon, A., Crépieux, P., and Reiter, E. (2015) Assessing Gonadotropin Receptor Function by Resonance Energy Transfer-Based Assays. *Front. Endocrinol. (Lausanne)*. 6, 1–14.

(39) Casarini, L., Lispi, M., Longobardi, S., Milosa, F., la Marca, A., Tagliasacchi, D., Pignatti, E., and Simoni, M. (2012) LH and hCG Action on the Same Receptor Results in Quantitatively and Qualitatively Different Intracellular Signalling. *PLoS One* 7.

(40) Riccetti, L., De Pascali, F., Gilioli, L., Potì, F., Giva, L. B., Marino, M., Tagliavini, S., Trenti, T., Fanelli, F., Mezzullo, M., Pagotto, U., Simoni, M., and Casarini, L. (2017) Human LH and hCG stimulate differently the early signalling pathways but result in equal testosterone synthesis in mouse Leydig cells in vitro. *Reprod. Biol. Endocrinol.* 15, 1–12.

(41) Di Rocco, G., Bernini, F., Borsari, M., Martinelli, I., Bortolotti, C. A., Battistuzzi, G., Ranieri, A., Caselli, M., Sola, M., and Ponterini, G. (2016) Excitation-energy transfer paths from tryptophans to coordinated copper ions in engineered azurins: A source of observables for monitoring protein structural changes. *Zeitschrift fur Phys. Chemie* 230, 1329–1349.

(42) Scipioni, A., Stefanini, Æ. S., and Santone, Æ. R. (2005) Immunohistochemical localisation of PDE5 in Leydig and myoid cells of prepuberal and adult rat testis 401–407.

(43) Santi, D., Spaggiari G., Casarini L., Fanelli F., Mezzuolo M., Pagotto U., Granata ARM., Carani C., S. M. (2017) Central hypogonadism due to a giant, “silent” FSH-secreting, atypical pituitary adenoma: effects of adenoma dissection and short-term Leydig cell stimulation by luteinizing hormone (LH) and human chorionic gonadotropin (hCG). *Aging Male* 20, 96–101.

(44) Dunkern, T. R., and Hatzelmann, A. (2005) The effect of Sildenafil on human platelet secretory function is controlled by a complex interplay between phosphodiesterases 2, 3 and 5 17, 331–339.

(45) Stief, C. G., Ückert, S., Becker, A. J., Harringer, W., Truss, M. C., Forssmann, W. G., and Jonas, U. (2000) Effects of sildenafil on cAMP and cGMP levels in isolated human cavernous and cardiac tissue. *Urology* 55, 146–150.

(46) Lofrano-Porto, A., Barra, G. B., Giacomini, L. A., Nascimento, P. P., Latronico, A. C., Casulari, A., De Assis Da, F., and Neves, R. (2007) Luteinizing Hormone Beta Mutation and Hypogonadism in Men and Women. *N Engl J Med* 357, 897–904.

(47) Andric, S. A., Janjic, M. M., Stojkov, N. J., and Kostic, T. S. (2010) Testosterone-Induced Modulation of Nitric Oxide-cGMP Signaling Pathway and Androgenesis in the Rat Leydig Cells1. *Biol. Reprod.* 83, 434–442.

(48) Casarini L, Santi D, Simoni M, P. F. (2018) ‘Spare’ Luteinizing Hormone Receptors: Facts and Fiction. *Trends Endocrinol. Metab.* 29, 208–217.

(49) Casarini, L., Riccetti, L., Pascali, F. De, Gilioli, L., Marino, M., Vecchi, E., Morini, D., Nicoli, A., Battista, G., and Sala, L. (2017) Estrogen Modulates Specific Life and Death Signals Induced by LH and hCG in Human Primary Granulosa Cells In Vitro.

(50) Sokanovic, S. J., Baburski, A. Z., Janjic, M. M., Stojkov, N. J., Bjelic, M. M., Lalošević, D., Andric, S. A., Stojilkovic, S. S., and Kostic, T. S. (2013) The opposing roles of nitric oxide and cGMP in the age-associated decline in rat testicular steroidogenesis. *Endocrinology* 154, 3914–3924.

(51) Huang, M., Lee, K. J., Kim, K., Ahn, M. K., Cho, C., Kim, D. H., and Lee, E. H. (2016) The maintenance ability and Ca²⁺ availability of skeletal muscle are enhanced by sildenafil.